Temperature-Jump Investigations of the Kinetics of Hydrogel Nanoparticle Volume Phase Transitions

Jianping Wang,[†,‡] Daoji Gan,[†] L. Andrew Lyon,*[,†] and Mostafa A. El-Sayed*[,†,‡]

Contribution from the Laser Dynamics Laboratory and School of Chemistry and Biochemistry, Georgia Institute of Technology, Atlanta, Georgia 30332-0400

Received July 13, 2001

Abstract: The dynamics of the deswelling and swelling processes in thermoresponsive poly-*N*-isopropylacrylamide (pNIPAm) hydrogel nanoparticles have been studied by using time-resolved transmittance measurements, in combination with a nanosecond laser-induced temperature-jump (T-jump) technique. A decrease in the solution transmittance associated with deswelling of the particles has been observed as the solution temperature traverses the volume phase transition temperature of the particles. Upon inducing the T-jump, the deswelling transition only occurs in a small percentage (<10%) of the particle volume, which was found to be a thin periphery layer of the particles. The particle deswelling occurs on the microsecond time scale, and as shown previously, the collapse time can be tuned via adding small amounts of hydrophobic component to the particle shell. In contrast, the reswelling of the particles was thermodynamically controlled by bath equilibration, and only small differences in particle reswelling kinetics were found due to sluggish heat dissipation (millisecond time scale) from the sample cell.

Introduction

Colloidal microgel particles[1] composed of environmentally responsive polymers such as poly-*N*-isopropylacrylamide (pNIPAm) possess a combination of unique properties, which make them attractive candidates for a number of potential applications in fields such as drug delivery,[2−4] biosensing,[5] soft actuators/valves,[6] and catalysis.[7] The specifics of these property changes result from phase separation of the polymer from the solvent in response to an environmental stimulus. For example, in the case of lightly cross-linked pNIPAm particles, as the temperature increases above a volume phase transition temperature (VPTT, ∼32 °C), the polymer gels undergo a reversible deswelling event due to dissociation of water molecules from the polymer chains and concomitant polymer self-association. Associated with this transition are large modulations of properties such as particle hydrophobicity,[8] size,[9,10] porosity, refractive index, colloidal stability, scattering cross-section,[11,12] electrophoretic mobility,[13−15] and rheology.[16,17]

This behavior has stimulated numerous fundamental studies of both the thermodynamics and kinetics of volume phase transitions.[18−22] While much of the early work in this area was devoted to lower critical solution temperature (LCST) behavior of macroscopic gels or solutions of the linear polymer, attention has been turned more recently to the study of spherical microgels. From the standpoint of VPT thermodynamics, large strides have been made in both experimental and theoretical studies of the (continuous) phase transitions observed for microgels.[1,23−29] These pseudo-first-order transitions stand in stark contrast to the sharp discontinuities observed for many macroscopic gels with apparently identical chemical structures,[22] and have therefore been a topic of some interest. However, it is now clear from numerous studies that a radial gradient in

* To whom correspondence should be addressed: lyon@chemistry.gatech.edu and mostafa.el-sayed@chemistry.gatech.edu.
† School of Chemistry and Biochemistry
‡ Laser Dynamics Laboratory

(1) Pelton, R. *Adv. Colloid. Interface Sci.* **2000**, *85*, 1−33.
(2) Park, T. G. *Biomaterials* **1999**, *20*, 517−521.
(3) Makino, K.; Hiyoshi, J.; Ohshima, H. *Colloids Surf., B* **2001**, *20*, 341−346.
(4) Ichikawa, H.; Fukumori, Y. *J. Controlled Release* **2000**, *63*, 107−119.
(5) Holtz, J. H.; Asher, S. A. *Nature* **1997**, *389*, 829−832.
(6) Beebe, D. J.; Moore, J. S.; Bauer, J. M.; Yu, Q.; Liu, R. H.; Devadoss, C.; Jo, B. H. *Nature* **2000**, *404*, 588−590.
(7) Bergbreiter, D. E.; Case, B. L.; Liu, Y.-S.; Caraway, J. W. *Macromolecules* **1998**, *31*, 6053−6062.
(8) Kawaguchi, H.; Fujimoto, K.; Mizuhara, Y. *Colloid Polym. Sci.* **1992**, *270*, 53−57.
(9) Saunders, B. R.; Vincent, B. *J. Chem. Soc., Faraday Trans.* **1996**, *92*, 3385−3389.
(10) Saunders, B. R.; Crowther, H. M.; Morris, G. E.; Mears, S. J.; Cosgrove, T.; Vincent, B. *Colloid Surf. A-Physicochem. Eng. Asp.* **1999**, *149*, 57−64.
(11) Yi, Y. D.; Oh, K. S.; Bae, Y. C. *Polymer* **1997**, *38*, 3471−3476.
(12) Yi, Y. D.; Bae, Y. C. *J. Appl. Polym. Sci.* **1998**, *67*, 2087−2092.
(13) Rasmusson, M.; Vincent, B.; Marston, N. *Colloid Polym. Sci.* **2000**, *278*, 253−258.
(14) Fernandez-Nieves, A.; Fernandez-Barbero, A.; de las Nieves, F. J.; Vincent, B. *J. Phys.-Condes. Matter* **2000**, *12*, 3605−3614.
(15) Fernandez-Nieves, A.; Fernandez-Barbero, A.; Vincent, B.; de las Nieves, F. J. *Macromolecules* **2000**, *33*, 2114−2118.
(16) Senff, H.; Richtering, W.; Norhausen, C.; Weiss, A.; Ballauff, M. *Langmuir* **1999**, *15*, 102−106.
(17) Senff, H.; Richtering, W. *J. Chem. Phys.* **1999**, *111*, 1705−1711.
(18) Tanaka, T.; Fillmore, D. J. *J. Chem. Phys.* **1979**, *70*, 1214−1218.
(19) Li, Y.; Tanaka, T. *J. Chem. Phys.* **1990**, *92*, 1365−1371.
(20) Annaka, M.; Tanaka, T. *Nature* **1992**, *355*, 430−432.
(21) Tanaka, T.; Fillmore, D. J.; Sun, S.-T.; Nishio, I.; Swislow, G.; Shah, A. *Phys. Rev. Lett.* **1980**, *45*, 1636−1639.
(22) Shibayama, M.; Tanaka, T. In *Advances in Polymer Science*; Springer-Verlag: Berlin, 1993; Vol. 109, pp 1−62.
(23) Wu, X.; Pelton, R. H.; Hamielec, A. E.; Woods, D. R.; McPhee, W. *Colloid Polym. Sci.* **1994**, *272*, 467−477.
(24) Wu, C.; Zhou, S. *Macromolecules* **1997**, *30*, 574−576.
(25) Wu, C. *Polymer* **1998**, *39*, 4609−4619.
(26) Duracher, D.; Elaissari, A.; Pichot, C. *Colloid Polym. Sci.* **1999**, *277*, 905−913.
(27) Wang, X.; Wu, C. *Macromolecules* **1999**, *32*, 4299−4301.
(28) Guillermo, A.; Addad, J. P. C.; Bazile, J. P.; Duracher, D.; Elaissari, A.; Pichot, C. *J. Polym. Sci. Pt. B−Polym. Phys.* **2000**, *38*, 889−898.
(29) Duracher, D.; Elaissari, A.; Pichot, C. *Macromol. Symp.* **2000**, *150*, 305−311.

10.1021/ja016610w CCC: $20.00
Published on Web 10/20/2001

cross-linker concentration exists in microgels prepared by precipitation polymerization,[23,28−31] and that this gradient is responsible for a gradient in the free energy of polymer deswelling.[24,25,31] Specifically, fluorescence[31] and NMR[28] experiments have been designed to probe such heterogeneity, and have clearly illustrated that the core of swollen pNIPAm microgels contains a higher cross-link density than the particle periphery. This gradient apparently arises from the faster rate of cross-linker incorporation into the microgel than other monomers in solution, where rapid incorporation of cross-linker results in a dense seed particle upon which more loosely cross-linked material is polymerized. It is interesting to note that the cross-linker used in these studies (*N,N′*-methylenebis(acrylamide), BIS) is more hydrophilic than pNIPAm at temperatures above the VPTT. Contrary to the experimentally observed gradient, it might therefore be expected that the cross-linker-rich phase would partition to the particle *surface* during polymerization, thereby producing a higher cross-linker concentration at the particle periphery. However, highly cross-linked networks have, by definition, lower mobility than loosely cross-linked systems, and should therefore not be able to continually partition to the particle surface. We have shown previously that 5 mol % cross-linking is sufficient to limit the degree of interpenetration in core−shell microgels,[31,32] suggesting that the low mobility of moderately cross-linked networks limits their ability to phase separate significantly. As mentioned above, this gradient should have a profound influence on the mechanism of microgel collapse,[24,25] as it has been demonstrated that the longer polymer chains in a thermoresponsive network undergo a phase separation event at lower temperatures than the shorter (more highly cross-linked) chains. One can therefore show in a thermodynamically rigorous fashion that the pNIPAm particle periphery undergoes a phase separation at lower temperatures than the particle core, because of a higher degree of cross-linking at the interior of the particle.

VPT kinetics have also been studied extensively. In studies of macroscopic gels, Tanaka et al. showed that the transition rate was inversely proportional to the square of the smallest dimension of the material.[18,19,33] Therefore, in comparison to the macrogels that may take hours or days to respond to an environmental change, microgels exhibit a very rapid response that cannot be followed by the typical visual inspection methods employed for larger structures. In a previous article, we studied the kinetics of microgel VPTs via differential scanning calorimetry (DSC), wherein we took advantage of the *thermodynamic* radial collapse mechanism discussed above to affect large changes in the deswelling *kinetics* via small chemical modifications made to the particle periphery. In this contribution, we describe the first application of temperature-jump time-resolved visible transmittance spectroscopy, which has previously been applied to protein folding studies, to interrogate the deswelling kinetics of pNIPAm microgels.

Experimental Section

Materials and Polymerization. *N*-Isopropylacrylamide (NIPAm) was obtained from Aldrich and recrystallized from hexane (J. T. Baker) before use. Both butyl methacrylate (BMA) and *N,N*-dimethylformamide (DMF) (Aldrich) were distilled under reduced pressure. *N,N′*-Methylenebis(acrylamide) (BIS), sodium dodecyl sulfate (SDS) ,and ammonium persulfate (APS) were used as received from Aldrich. Water used in all syntheses and measurements was distilled and then purified with use of a Barnstead E-Pure system operating at a resistance of 18 MΩ. A 0.2 μm filter incorporated into this system removed particulate matter. A detailed procedure for the preparation of pNIPAm core and core−shell nanoparticles by free radical precipitation polymerization is described in detail elsewhere.[31,32,34] To briefly summarize the synthesis, core particles were synthesized from various ratios of NIPAm, BMA (if desired) predissolved in DMF at a concentration of 5 mg/mL, BIS, and SDS, in 150 mL of nitrogen-purged water. The reaction mixture was kept at 70 °C under a stream of nitrogen for 2 h. Following the addition of APS, the polymerization was carried out at 70 °C for 6 h under a nitrogen atmosphere. In cases where chemical differentiation was required at the particle periphery, this first batch of hydrogel particles (core) served as nuclei in a second stage of polymerization (shell addition). In the shell synthesis, a solution of the desired core particles was heated to 70 °C, whereupon a feed of NIPAm, BMA, BIS, SDS, and degassed water was introduced to the reaction flask. This solution was kept at 70 °C under a stream of nitrogen for 2 h. Polymerization was then initiated by the addition of APS; polymerization was again carried out for 6 h. All core−shell particles were purified via dialysis. It should be noted that under these synthesis conditions, the core particles are deswollen polymer globules, while the monomers are soluble in the continuous phase. Therefore, the degree of core swelling by monomer is very minimal, resulting in a low degree of interpenetration of the core and shell during shell addition. Furthermore, the relatively high level of cross-linking (typically 5 mol %) tends to limit the degree of interpenetration when the particles cool and reswell.[31,32] To minimize the effects of variable core sizes on the thermodynamic and kinetic measurements, within the particle series (CS1−CS5) the same batch of core particles was used to construct the core−shell particles. This is reflected by the consistent core sizes within that series, as shown in Table 1. The approximate particle sizes were controlled by varying the concentration of SDS during polymerization. In general, higher concentrations of SDS result in smaller particle sizes, as predicted by homogeneous nucleation theory.[23,35] The chemical compositions and mean equilibrium swelling radii of the hydrogel particles are listed in Table 1.

Table 1. Chemical Compositions, Radii, and T-Jump-Induced Deswelling Time (τ) of pNIPAm Particles

	core			shell			
	BMA (to NIPAm %)			BMA (to NIPAm %)			
sample[a]	feed	obsd[b]	$R_{core-shell}$[c] (nm)	feed	obsd[b]	$R_{core-shell}$[c] (nm)	τ, μs[d]
C1			201				0.39 ± 0.08
C2			150				0.41 ± 0.09
C3			108				0.23 ± 0.03
C4			97				0.22 ± 0.03
C5			50				0.30 ± 0.06
CS	1.00	0.92	137	1.00	0.89	195	0.88 ± 0.07
CS1			147			206	0.45 ± 0.06
CS2			147	0.50	0.46	210	0.67 ± 0.07
CS3			147	1.00	0.94	194	0.93 ± 0.07
CS4			147	1.50	1.40	193	1.0 ± 0.1
CS5			147	2.00	1.87	197	1.5 ± 0.1

[a] All the particles were synthesized with 5 mol % (based on NIPAm) BIS as a cross-linker; [b] Observed by ^{1}H NMR in $CDCl_3$. [c] Particle radii measured by PCS at 25 °C. [d] Average of 3 replicated measurements of particle deswelling time upon laser-induced T-jump.

Photon Correlation Spectroscopy. Mean particle sizes and particle size distributions were determined with use of a photon correlation spectrometer (PCS) (Protein Solutions, Inc.) with a programmable temperature controller, as described previously.[31,32,34,36]

Temperature-Jump (T-Jump) Apparatus. The details of the T-jump apparatus have been described previously.[37] Briefly, the

(30) Gilanyi, T.; Varga, I.; Meszaros, R.; Filipcsei, G.; Zrinyi, M. *Phys. Chem. Chem. Phys.* **2000**, *2*, 1973−1977.
(31) Gan, D.; Lyon, L. A. *J. Am. Chem. Soc.* **2001**, *123*, 8203−8209.
(32) Jones, C. D.; Lyon, L. A. *Macromolecules* **2000**, *33*, 8301−8306.
(33) Matsuo, E. S.; Tanaka, T. *J. Chem. Phys.* **1988**, *89*, 1695−1703.
(34) Gan, D.; Lyon, L. A. *J. Am. Chem. Soc.* **2001**, *123*, 7511−7517.
(35) McPhee, W.; Tam, K. C.; Pelton, R. *J. Colloid Interface Sci.* **1993**, *156*, 24−30.
(36) Debord, J. D.; Lyon, L. A. *J. Phys. Chem. B* **2000**, *104*, 6327−6331.
(37) Wang, J.; El-Sayed, M. A. *Biophys. J.* **1999**, *76*, 2777−2783.

fundamental output at 1064 nm of a Nd:YAG laser (Quantum-Ray DCR-3) was focused into a Raman cell (stainless steel tube with quartz windows, 85 cm in length and 32 mm in diameter, filled with 200 − 300 psi H_2). This produced a heating pulse at 1.9 μm (10-ns pulse width, 6−8 mJ/pulse at 10 Hz) for the T-jump experiment. This heating pulse was absorbed by the overtone of the O−D stretching vibration of D_2O (solvent), a weak absorption centered at $\sim$ 5240 cm^{-1}. A 100 μm path-length IR cell with two CaF_2 plates and a Teflon spacer was used to give the effective sample heating volume of 1 $mm^2 \times 100\ \mu$m. The resultant T-jump is $\sim$10 °C,[37] and the temperature reaches its maximum value within $\sim$20 ns (twice the laser pulse width) since the thermalization and diffusion within water (D_2O) is a subnanosecond event,[38] whereas the cooling time of the T-jump system is in the order of tens of milliseconds. The sample cell was temperature controlled at 30 °C by using a thermostated bath system (RET-100, NESLAB Instruments, Inc., Union City, CA), and the system was thermally stabilized at least 20 min before applying the T-jump pulse.

Time-Resolved Visible Transmittance Spectroscopy. In this experiment, a CW He−Ne laser operating at 633 nm with an output power of 10 mW was used as the probe beam. A fast silicon photodiode with 10-ns response time was used to monitor the transmittance change of the pNIPAm/D_2O (3 mg/mL) solution with or without the external perturbation (T-jump). To ensure that particle diffusion out of the probe beam did not complicate analysis, the overlapping pump beam was more than 2-fold larger in diameter than the probe (pump $\sim$2-mm diameter, probe <1-mm diameter). Thus, the rate of diffusion of thermally excited particles in to and out of the probe beam was practically equivalent on the experimental time scale. In addition, the diffusion of particles out of the pump beam before completion of the monitored events should be insignificant, given the size of the beam and the slow diffusion of $\sim$400-nm diameter particles.

Data acquisition was triggered by a Q-switch of the YAG laser, and recorded by using a 500 MHz oscilloscope digitizer (Lecroy 9350A). The heating pulse appeared at a delay time of about 75 ns after the Q-Switch. The RF-pickup noise on the Si-photodiode was subtracted as the background. One thousand laser shots were averaged to improve the signal-to-noise ratio of transient signals. The Nd:Yag laser light and the CW He−Ne laser light overlapped on to the sample cell with a beam size of <1 mm^2. The exposed part of the sample was changed to a new position every 1000 laser shots. Sample damage was found to be negligible in 1−2 h experimental time.

Results and Discussion

pNIPAm microgels were prepared via free radical precipitation polymerization to produce size-controlled, monodispersed spherical nanoparticles, as reported previously.[31,32,34,36] Typical photon correlation spectroscopy (PCS) measurements of pNIPAm microgels in D_2O are shown in Figure 1 as a function of temperature. The measurements were taken under equilibrium conditions after holding the sample for 10 min at each temperature (prolonged equilibration times do not lead to differences in the observed behavior). The transition temperature ($\sim$34 °C), which is defined here as the midpoint in the transition curve, is about 1 °C higher than that measured in water (H_2O) solution, but the shapes of both transition curves are quite similar (Supporting Information, S1). The slight shift of the LCST to a higher temperature has also been observed previously for linear pNIPAm in D_2O.[27] Accompanying the decrease in the particle size, the relative turbidity of the solution, which is calculated by comparing the PCS observed scattered light intensity at the measured temperature with the maximum observed intensity (at 41 °C), sharply increases as the solution temperature is raised above the VPTT. This increase in particle scattering cross-section occurs despite the smaller particle size due to the large increase in particle refractive index. In the fully swollen form, the particle is nearly index-matched to the solvent; at the VPTT water expulsion results in a sudden increase in the *difference* in refractive index between the solvent and the particle, and hence yields a highly turbid solution. The small, random fluctuations in the measured polydispersity below the maximum value of $\sim$17% suggest that the particles are monodispersed and do not form aggregates as the solution temperature is raised above the VPTT. It is worth mentioning that the curves of the particle size and turbidity versus temperature are nearly symmetric, with the same sharpness and breadth. Therefore, assuming that a temperature-jump (T-jump) measurement probes the same reaction path that is interrogated in the equilibrium measurements, the change in solution turbidity should be a direct measure of the particle size change. Taking advantage of this effect, we measured the change of the solution transmittance upon inducing a T-jump across the VPTT to probe the kinetics of particle deswelling.

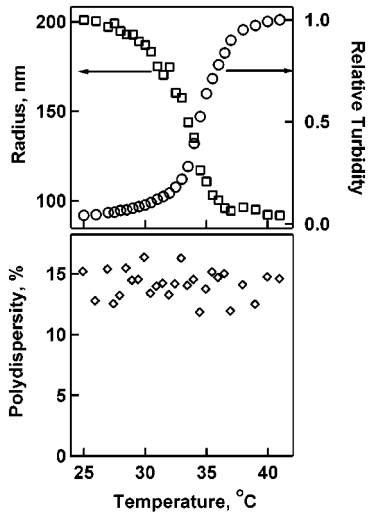

Figure 1. (a) Hydrodynamic radius (squares) and solution relative turbidity (circles) and (b) sample polydispersity of pNIPAm particles (Sample C1) as a function of temperature as measured by PCS under thermal equilibrium in D_2O.

To induce a T-jump in a solution of pNIPAm particles on nanosecond time scale, freeze-dried microgel samples were redispersed in D_2O at a concentration of 3 mg/mL, and a heating pulse centered at 1.9 μm (an energy where the polymer is transparent but D_2O is absorptive) was employed. The initial temperature was thermostated at 30 °C, just below the volume phase transition temperature ($\sim$34 °C) of the hydrogel nanoparticles. Upon introduction of the IR laser pulse, a temperature jump of $\sim$10 °C is induced within the first 20 ns,[37] thereby causing the local temperature to rise above the transition temperature of the hydrogel particles. Figure 2 shows a typical time-dependence of the T-jump-induced transmittance change (observed at 633 nm) for pNIPAm particles in D_2O. A decrease in the solution transmittance is apparent approximately 600 ns after the introduction of the laser pulse. It was found that the transmittance change was absent or weaker if the initial temperature was set far below the phase transition temperature (e.g., 16 °C), as the T-jump did not traverse or only partially traversed the VPTT. Furthermore, introduction of a T-jump to a system containing solvent (D_2O) only did not produce a transmittance change above the instrumental noise, suggesting that the solvent contributes negligibly to the observed transmittance change. Accordingly, the observed decrease in the transmittance can be attributed to an increase in the solution turbidity associated with the deswelling of the hydrogel particles.

(38) Williams, S.; Causgrove, T. P.; Gilmanshin, R.; Fang, K. S.; Callender, R. H.; Woodruff, W. H.; Dyer, R. B. *Biochemistry* **1996**, *35*, 5, 691−697.

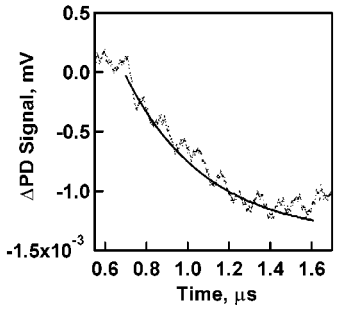

Figure 2. Representative time-dependence of the T-jump-induced transmittance change observed at 633 nm of pNIPAm microgel (Sample C1) in D_2O. A decrease in the transmittance signal (photodiode voltage) was observed 620 ns after the initial heating pulse. The particle collapse process can be fit to a single-exponential decay, with a formation time, τ, of 0.39 μs.

Curve fitting of the transmittance change shows a single-exponential process, with an apparent formation time (τ) of ~0.39 μs.

The rather long delay time between the onset of the transmittance change and the heating pulse suggests that the hydrogel particles take ~600 ns to respond to the T-jump, while the solvent responds much more quickly. This delay time of the pNIPAm hydrogel is expected, given the intrinsic thermal conductivity properties of the hydrogel. Similar situations have been observed in other systems such as protein solutions, where a protein unfolding event displayed a ~1 ns delay, despite the fact that the laser-induced T-jump was introduced within 30 ps.[39] It has also been observed that a ~300 ns delay accompanies the dissociation of water from the interior hydrophobic domains of bacteriorhodopsin.[37] In the present system, the hydrogel deswelling event requires heating of the D_2O that solvates the hydrogel network, followed by dissociation of D_2O from the polymer chains. To heat the D_2O contained inside the hydrogel, it is expected that the thermal energy will be transferred from the bath solvent (that which is not entrained inside the microgels) to the D_2O that solvates the polymer network. It should be noted that the tightly bound, polymer-solvating D_2O should not have the same optical frequency as the D_2O in the continuous phase and should therefore not be subject to the same degree of heating by the T-jump pulse. Furthermore, the thermal conductivity of dilute polyacrylamide solutions has been measured to be ~0.05 W m^{-1} K^{-1} [40] and is a decreasing function with increasing polymer concentration. Therefore, the higher local concentration of polymer in a microgel should result in much greater than 12-fold decrease in thermal conductivity than that of D_2O alone (~0.60 W m^{-1} K^{-1}).[41] From this it is apparent that the heating and dissociation of D_2O involved in polymer solvation can reasonably be assumed to occur on a much longer time scale than the heating of free D_2O, thereby leading to a long lag time between solvent heating and hydrogel response.

To interrogate the influence of particle volume on collapse rate, a series of pNIPAm particles (C1−C5) with various sizes (radii varying from ~50 to 200 nm) were synthesized containing a 5 mol % cross-linking density (Table 1). PCS measurements under thermal equilibrium conditions show that all five samples display identical VPT behavior (Supporting Information, S2),

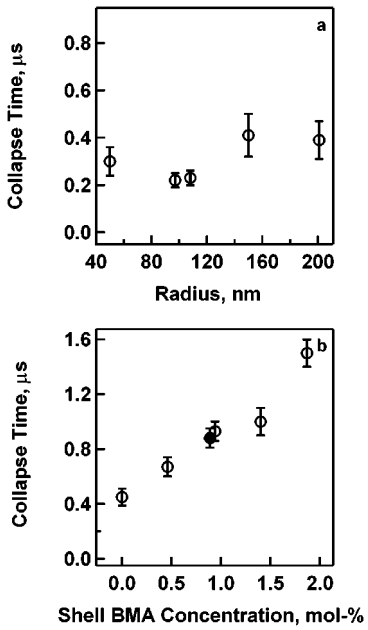

Figure 3. (a) Dependence of the collapse time, τ, on the radius of the pNIPAm hydrogel nanoparticle. (b) Dependence of the collapse time on the BMA shell concentration for a series of pNIPAm (core)/pNIPAm-*co*-BMA (shell). The black data point represents sample CS, which contained equal concentrations (1 mol %) of BMA in both the core and shell. Details of the particle compositions are listed in Table 1.

making it appropriate to use the same initial temperature and laser pulse for each particle. Figure 3a shows the T-jump induced collapse time (τ) as a function of the particle size for this series. Despite the fact that the square of the particle radius varies 16-fold over this range of sizes, the collapse time displays no strong trend with particle radius and shows only small fluctuations between 0.2 and 0.4 μs. These results suggest that no significant dependence of collapse rate on microgel size exists, directly contradicting both the fundamental theory of VPT kinetics[18] and differential scanning calorimetry (DSC) measurements,[34] which show that the overall collapse time is proportional to the square of the gel radius.

This apparent contradiction is easily explained, however, when one considers the actual degree to which deswelling occurs in these experiments. In the steady state PCS measurements shown in Figure 1, a large change in solution turbidity is observed upon crossing the VPTT. However, the change in transmittance shown in Figure 2 is only on the order of 0.15% of the initial probe laser intensity. A much larger change in transmittance would be expected for complete particle deswelling given the steady state results. Therefore it appears that only partial collapse of the microgels is taking place following the T-jump. This is not unexpected, given that the solution temperature jump of ~10 °C occurs in less than 20 ns, while the microgel takes ~600 ns to attain the elevated temperature. These differences in thermal conductivity and equilibration time scales will limit the degree to which the microgel is thermally excited and therefore will limit the extent of deswelling. To more accurately estimate the deswelling level of the particles, the static transmittance was determined at both 30 and 40 °C to obtain the transmittance change associated with 100% deswelling. Upon comparison of this transmittance difference with those obtained from the time-resolved measurements, it was found that the T-jump induced transmittance change corresponded to only 3−4% of the static transmittance difference, despite the apparent temperature differences in both

(39) Phillips, C. M.; Mizutani, Y.; Hochstrasser, R. M. *Proc. Natl. Acad. Sci. U.S.A.* **1995**, *92*, 7292−7296.
(40) Osman, M. B.; Dakroury, A. Z.; Mokhtar, S. M. *Polym. Bull.* **1992**, *28*, 181−188.
(41) Vargaftik, N. B.; Vinogradov, Y. K.; Yargin, V. S. In *Handbook of physical properties of liquids and gases: pure substances and mixtures*, 3rd ed.; Begell House: New York, 1996; p 145.

experiments being identical. This suggests, in turn, that a very small portion of the particle is subject to deswelling events in these T-jump experiments. As described above, pNIPAm microgels have a heterogeneous structure with a decreasing gradient in cross-linking density from the center to the periphery,[28,31] which results in the VPTT of the particle periphery being lower than that of the core.[24,25,31] Furthermore, since the continuous phase (D_2O solvent) reaches its maximum temperature faster than the particles, the portion of the particle that equilibrates with the solvent first should lie at the periphery. Therefore, it is reasonable to assume that the collapse of the particles starts from the microgel periphery in a T-jump measurement, and that in our case the portion of the particle that initially undergoes collapse is isolated to a peripheral outer shell.

This argument also assists in the explanation of the magnitude of the hydrogel collapse times. For a 200-nm radius particle, one can make a reasonable estimate of the expected collapse kinetics. For example, Shibayama et al. have measured the collective gel diffusion coefficient (which takes into account solvent diffusion, polymer chain motion, and polymer friction) for macroscopic pNIPAm gels to be on the order of 2×10^{-7} cm^2 s^{-1}.[42] If we assume that this value scales to the submicron scale, we can estimate the collapse time of a 200-nm radius gel to be ~2 ms. Obviously, the 350 ns collapse time described above is far faster than that expected given the macroscopic gel diffusion rates. Yet if we consider that the turbidity data suggest that only a small outer portion of the particle is affected by the T-jump, we find that the predicted collapse rate would be closer to 3 μs. While this value is closer to the measured collapse time, it is still almost an order of magnitude different from the expected value. However, it should be noted that the measurement of collapse rates of macroscopic gels is often complicated by the presence of severe mechanical instabilities and phase separation during gel collapse.[42] It is quite probable that such instabilities do not exist at the loosely cross-linked exterior of microgels, thereby making the gel diffusion rate somewhat faster than that for macroscopic gels. Nonetheless, it is quite probable, given the results shown above, that the T-jump measurements presented here are only interrogating the early stages of collapse at the particle periphery, and do not probe the microgel collapse as a whole.

Our previous work on kinetic tuning of core−shell particles showed that localization of low concentrations of a hydrophobic monomer in the particle shell resulted in large modulation of the collapse kinetics.[34] Specifically, introduction of trace amounts of the hydrophobic monomer butyl methacrylate (BMA) into the periphery of pNIPAm particles did not change the observed VPTT, but produced large magnitude changes in the particle deswelling kinetics as measured by nonequilibrium DSC.[34] In that work, it was hypothesized that the localization of the hydrophobe at the periphery was sufficient to produce changes in the collapse kinetics because the initial (thermodynamic and kinetic) stages of the VPT took place in the particle shell. The early stages of collapse would then result in the formation of a very thin, semipermeable skin layer, corresponding to the formation of a dehydrated shell of polymer surrounding a hydrated core. The hydrophobicity of this skin layer then tunes the diffusion rate of water from the shell and subsequently from the particle interior. As further deswelling occurs, the dehydrated layer thickens, and a decrease in the particle size is observed. Skin layer formation is typically observed for macroscopic gels prepared by bulk polymerization,[42−46] where a thin layer of dense, collapsed polymer network forms on the gel surface following a temperature jump across the VPT. In the case of macrogels, this is an unstable, nonequilibrium state, as the positive osmotic pressure in the gel interior eventually breaks down the skin layer and allows further expulsion of water from the polymer. Apparently, the microgel analogue of this event does not involve gel rupture, as it is generally considered that microgels can be reversibly cycled across their VPTT without loss of structural integrity. Despite the subtle differences in skin layer formation between macro- and microgels, a strong kinetic modulation was observed in our previous studies, which attributed to the formation of a hydrogel skin. It is interesting to note that this modulation is present even though the deswollen hydrogel still may contain up to 20% water by volume following the phase separation.[17,47] Therefore, the skin layer should still have some degree of porosity that allows for water expulsion. Nonetheless, it is apparent that strong kinetic modulation can be accomplished by chemical modification of the skin.[34]

To corroborate these results, we applied the T-jump method to measure the VPT kinetics of hydrophobically modified pNIPAm core−shell particles. The chemical compositions of a series of such particles, the synthesis and characterization of which have been reported previously,[34] are shown in Table 1. In contrast to the relative lack of particle size dependence on the rate (Figure 3a), T-jump measurements of these samples showed a large increase in the collapse time with increases in the concentration of BMA into the shell layer of the core−shell hydrogel particles (Figure 3b). The collapse time of the core−shell hydrogel changed from 0.45 μs to 1.5 μs when 2 mol % BMA was introduced into the shell. However, introduction of the BMA component into the core does not have any added influence on the collapse time (Figure 3b and Table 1), as particles containing 1 mol % BMA in both the core and the shell (sample CS) show a collapse time similar to particles containing 0 mol % BMA in the core and 1 mol % BMA in the shell (sample CS3). These results agree strongly with those obtained previously by DSC. In those measurements, peak broadening of the DSC endotherm at a constant temperature ramp was related to the relative collapse rates; a linear 3-fold decrease in rate was observed upon increasing the BMA concentration from 0% to 2% and nearly identical kinetics were observed for samples CS and CS3. The good correlation between the complete collapse (DSC) and shell collapse (T-jump) results can be seen in Figure 4, where the DSC peak widths presented in our previous study are plotted against the T-jump obtained initial collapse times. For values up to 1.5 mol % BMA the correlation is extremely good, with the value for 2 mol % falling somewhat off of the line. Upon inspection of Figure 3, it can be seen that the 2 mol % value seems anomalously high on that plot as well. The origin of this deviation from linear behavior is at this time unknown and is the subject of continued investigations. One possible explanation, however, is that a concentration of 2 mol % BMA represents the point at which some small phase separation into BMA-rich phases occurs. The T-jump measurement may be more sensitive to a small amount of domain structure than the DSC measurement, thereby making

(42) Shibayama, M.; Nagai, K. *Macromolecules* **1999**, *32*, 7461−7468.
(43) Kaneko, Y.; Yoshida, R.; Sakai, K.; Sakurai, Y.; Okano, T. *J. Membr. Sci.* **1995**, *101*, 13−22.
(44) Suzuki, A.; Yoshikawa, S.; Bai, G. *J. Chem. Phys.* **1999**, *111*, 360−367.
(45) Yoshida, R.; Sakai, K.; Okano, T.; Sakurai, Y. *J. Biomater. Sci., Polym. Ed.* **1992**, *3*, 243−252.
(46) Hirokawa, Y.; Sato, E.; Hirotsu, S.; Tanaka, T. *Polym. Mater. Sci. Eng.* **1985**, *52*, 520−522.
(47) Senff, H.; Richtering, W. *Colloid Polym. Sci.* **2000**, *278*, 830−840.

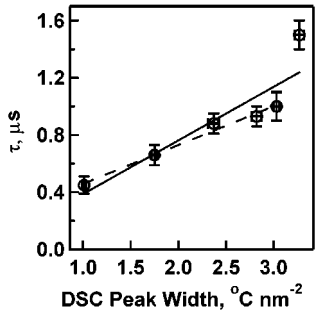

Figure 4. Plot of the T-jump measured collapse time, τ, versus the DSC measured peak width (from ref 34). The solid line represents a least-squares fit to the entire range of data, while the dashed line is a fit only to those data up to 1.5 mol % BMA.

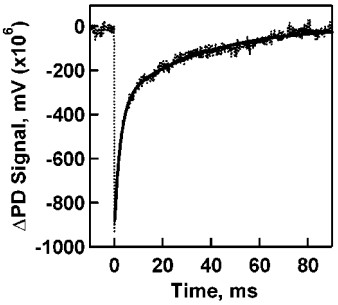

Figure 5. A typical relaxation process of the T-jump-induced transmittance change (photodiode voltage) in the time domain of 0−100 ms for a pNIPAm microgel (Sample C4) having a radius of 100 nm at 25 °C. The recovery process can be fit to a biexponential rise, with the two components being 2.6 (∼60% relative amplitude) and 35 ms (∼40% relative amplitude), respectively.

the correlation between the two techniques poor at that concentration. Nonetheless, the strong agreement at lower BMA concentrations between measurements of complete microgel collapse (DSC) and the T-jump measurements, which are mainly probing the initial (peripheral) stages of microgel deswelling, suggests that the rate-determining processes in microgel VPTs are mainly associated with the shell composition.

It is well-known that the phase transition of pNIPAm in water solution is a thermodynamically reversible process; deswollen pNIPAm particles reswell in water as the solution temperature is decreased below the VPTT.[1] To examine the relaxation process of the hydrogel particle, the T-jump induced transmittance change has also been followed on the tens of milliseconds time scale. Figure 5 shows a typical relaxation of the T-jump-induced transmittance change in the time domain of 0−100 ms. During this process, the system cools back to the thermostated temperature of 30 °C, thereby leading to reswelling of the hydrogel particles. The important information gained from these data is that the transmittance signal completely recovers to the original level, suggesting that the particles reswell to the original volume prior to the application of a second laser pulse. Thus signal averaging of the transient signal is valid, as the same initial state exists prior to the application of a T-jump. The recovery process can be mathematically described by a biexponential rise, with the lifetime and relative amplitudes being 2.6 (∼60%) and 35 ms (∼40%), respectively. For different samples, the lifetimes of these two processes have been found to fluctuate between 2 and 4 ms and 25−58 ms, respectively. No obvious correlation between these values and sample deswelling time existed. It is clear from this work and previous studies that the long recovery (reswelling) time is a function of the rate of heat dissipation from the system (sample cell, etc.),[37,38] which occurs on a much longer time scale than the VPT induced by the initial T-jump heating process. This assumption is further corroborated by a strong dependence of the recovery lifetimes on the volume of the pNIPAm/D_2O solution interrogated (controlled by the thickness of the cell spacer). Both components of the biexponential rise were found to increase with spacer thickness (solution volume), as a longer time was required to cool the larger solution volume.

Conclusions

The kinetics of pNIPAm microgel volume phase transitions have been measured via laser-induced T-jump measurements. The data suggest that under the current laser excitation conditions, only a very thin peripheral (shell) layer of the hydrogel particles is collapsed during the T-jump process. However, despite the relatively small volume change induced by the laser pulse, the relative deswelling kinetics agree very well with previous DSC studies for a series of hydrophobically shell-modified particles. Together, these results suggest that the initial stages of thermally induced microgel deswelling largely determine the rate of the collapse event, possibly due to the formation of a stable skin layer at the particle periphery, which limits the diffusion of water from the gel.

Acknowledgment. M.A.E. would like to thank the Chemical Sciences, Geosciences and Biosciences Division, Office of Basic Energy Sciences, Office of Sciences, U.S. Department of Energy (under grant DE-FG02-97ER14799) for financial support. L.A.L. gratefully acknowledges financial support from Research Corporation in the form of a Research Innovation Award, from the National Science Foundation for a CAREER Award, and from the Arnold and Mabel Beckman Foundation for a Young Investigator Award.

Supporting Information Available: S1, PCS measurements of sample C1 in H_2O and D_2O as a function of temperature; S2, radii and deswelling ratios of C1−C5 as a function of temperature measured by PCS in water solution; and S3−S4, representative deswelling transients for all samples listed in Table 1, with the exception of sample C1, which is shown in Figure 2, (PDF). This material is available free of charge via the Internet at http://pubs.acs.org.

JA016610W